ASTROBIOLOGY
Volume 4, Number 4, 2004
© Mary Ann Liebert, Inc.

Research Paper

Haze Aerosols in the Atmosphere of Early Earth: Manna from Heaven

MELISSA G. TRAINER,[1] ALEXANDER A. PAVLOV,[2] DANIEL B. CURTIS,[1] CHRISTOPHER P. MCKAY,[3] DOUGLAS R. WORSNOP,[4] ALICE E. DELIA,[5] DARIN W. TOOHEY,[5] OWEN B. TOON,[2,5] and MARGARET A. TOLBERT[1]

ABSTRACT

An organic haze layer in the upper atmosphere of Titan plays a crucial role in the atmospheric composition and climate of that moon. Such a haze layer may also have existed on the early Earth, providing an ultraviolet shield for greenhouse gases needed to warm the planet enough for life to arise and evolve. Despite the implications of such a haze layer, little is known about the organic material produced under early Earth conditions when both CO_2 and CH_4 may have been abundant in the atmosphere. For the first time, we experimentally demonstrate that organic haze can be generated in different CH_4/CO_2 ratios. Here, we show that haze aerosols are able to form at CH_4 mixing ratios of 1,000 ppmv, a level likely to be present on early Earth. In addition, we find that organic hazes will form at C/O ratios as low as 0.6, which is lower than the predicted value of unity. We also show that as the C/O ratio decreases, the organic particles produced are more oxidized and contain biologically labile compounds. After life arose, the haze may thus have provided food for biota. Key Words: Early Earth—Hydrocarbon aerosols—Atmospheric C/O ratio. Astrobiology 4, 409–419.

INTRODUCTION

THE WARMTH OF EARLY EARTH (Sagan and Mullen, 1972; Kasting, 1993) despite the faint young sun (Newman and Rood, 1977) suggests the primitive atmosphere contained potent greenhouse gases, which allowed for surface temperatures above the freezing point of water. Since the early 1980s it has been thought that this primitive atmosphere was oxidized, and contained large quantities of carbon dioxide (CO_2). Such an atmosphere would not be conducive to the formation of organic molecules, thus spurring an interest in the origin of life in specialized environments such as hot springs and the mid-ocean ridges, as well as the delivery of organic compounds from space. However, geologic evidence does not support high CO_2 levels in the anoxic Archean atmosphere (Rye *et al.,* 1995). Rather, it may have been that the early atmosphere was warmed by

[1]Department of Chemistry and Biochemistry and Cooperative Institute for Research in Environmental Sciences; [2]Laboratory for Atmospheric and Space Physics; and [5]Program in Atmospheric and Oceanic Sciences, University of Colorado at Boulder, Boulder, Colorado.
[3]Space Science Division, NASA Ames Research Center, Moffett Field, California.
[4]Aerodyne Research Inc., Billerica, Massachusetts.

methane (CH_4) as well as CO_2 (Kiehl and Dickinson, 1987; Pavlov *et al.*, 2000). The presence of global CH_4 would be more favorable to the formation of organic molecules and therefore the evolution of life (Miller and Schlesinger, 1984).

Methanogenic bacteria were likely one of the first microorganisms to have evolved on the Archean Earth, and would have provided a biological source of methane into the atmosphere (Woese, 1987). Photochemical simulations show that in an anoxic environment CH_4 can accumulate up to approximately 1,000 ppmv, provided the CH_4 source was close to present-day values (Pavlov *et al.*, 2001b). Even on the prebiotic Earth, CH_4 concentrations were likely to be quite high (Kress and McKay, 2004). An atmosphere containing moderate amounts of both CO_2 and CH_4 as greenhouse gases would have provided sufficient surface warming (Pavlov *et al.*, 2000) to raise the surface temperature of Earth above the freezing point of water.

With CH_4 levels of this magnitude, photochemical models suggest that photolysis of CH_4 would lead to the formation of an organic haze layer on the early Earth (Zahnle, 1986; Pavlov *et al.*, 2001a,b). On Saturn's moon, Titan, a reddish-brown haze layer, composed of solid organics, is formed by CH_4 photolysis as well as dissociation of nitrogen (N_2) and CH_4 by magnetospheric electrons and solar wind particles. Sagan and Chyba (1997) suggested that a similar organic haze layer on the early Earth would serve as an ultraviolet (UV) shield for the atmospheric components below, thus maintaining the CH_4 concentrations. However, the effectiveness of such a haze layer as a UV shield and the intensity of the antigreenhouse effect (which could negate any greenhouse effect provided by the CH_4) are highly dependent on the chemical and physical properties of the haze aerosol (McKay *et al.*, 1999; Pavlov *et al.*, 2000).

It is expected that on the early Earth, both the rate of production and the chemical composition of the haze would be affected by the oxidative capacity of the atmosphere. Models of haze formation in an early Earth context have focused on the atmospheric C/O ratio (Zahnle, 1986; Kasting, 1997; Pavlov *et al.*, 2000, 2001b). Because the photolysis of CO_2 produces O atoms that may terminate hydrocarbon chain production, the CO_2 might inhibit the formation of the haze aerosols. Figure 1 displays a reaction diagram that demonstrates a few expected pathways leading to particle formation. The reaction pathways for CH_4 and N_2 are given from modeling studies of Titan, and an expected effect of CO_2 inclusion is shown.

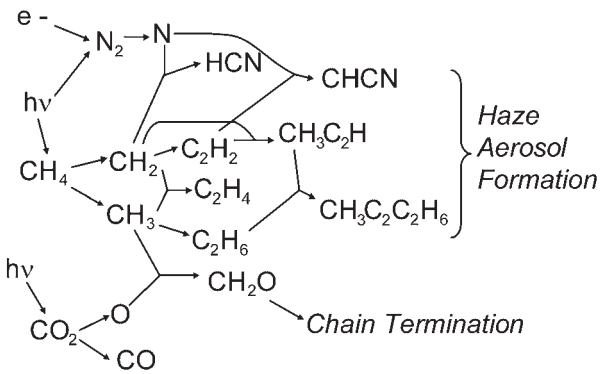

FIG. 1. Schematic diagram of a few suggested pathways for aerosol formation from N_2 and CH_4, with interference from CO_2 (Toublanc *et al.*, 1995; Pavlov *et al.*, 2001b).

With significant amounts of both CH_4 and CO_2, the ratio of C/O should dictate the type of reactions generated by photochemistry. Models typically conjecture that at C/O ratios exceeding unity, the CH_4 successfully polymerizes to form higher-order hydrocarbons. At lower C/O ratios, oxidation of CH_4 will likely hinder the polymerization process.

Although there has been recent modeling of haze formation under the conditions thought to have prevailed on early Earth, there has been little laboratory work on the topic. The majority of studies of planetary haze particles have been performed in Titan-like gaseous mixtures of 10% CH_4 in N_2, although some have gone to lower CH_4 concentrations (McDonald *et al.*, 1994; Thompson *et al.*, 1994). Because of the poor knowledge of the polymerization reactions for higher-order hydrocarbons, Pavlov *et al.* (2001b) numerically simulated production of C_5 and C_6 molecules only and considered it as the rate of organic haze formation. However, under typical Earth conditions, those molecules should have been present in the gaseous phase. Therefore, the predicted rate of haze formation can be inaccurate, and should be verified by experiment. Here, we describe new laboratory work to examine the formation and chemical composition of organic haze particles synthesized in an environment meant to simulate aspects of the early Earth's atmosphere, including likely CH_4 concentrations and variations in the C/O ratio.

Previous studies on planetary haze aerosols have typically involved collection and transfer of

the particles for later analysis. The aerosol products have then been studied with infrared spectroscopy, pyrolitic gas chromatography/mass spectrometry, electron microscopy, or elemental analysis (Sagan and Khare, 1979; Khare *et al.,* 1981, 1984; McDonald *et al.,* 1994; Coll *et al.,* 1995, 1999; McKay, 1996; de Vanssay *et al.,* 1999; Clarke *et al.,* 2000). A review of many of these results can be found in McKay *et al.* (2001). While in some such studies the aerosol has been successfully protected from exposure to laboratory air (Coll *et al.,* 1999; Khare *et al.,* 2002; Ramirez *et al.,* 2002), the majority of studies have shown evidence of significant oxidation and contamination of the product due to transfer of the particles for analysis. Experiments that involved *in situ* analysis have usually been limited to studying gas-phase products resulting from the synthesis (Thompson *et al.,* 1991; Coll *et al.,* 1995). To avoid this problem in our study, we developed a method by which we can analyze the aerosol products in real time, eliminating the possibility of contamination and removing the extensive times necessary for sample collection. We use an aerosol mass spectrometer (AMS) to study the chemical composition and size of particles in real time as a function of trace gas composition. In addition, we use a scanning mobility particle sizer (SMPS) as an alternate size analyzer, from which we can extract additional information about the physical properties of the aerosols.

MATERIALS AND METHODS

The experimental apparatus was based on previous designs for the production of Titan-like haze aerosols (Thompson *et al.,* 1991; Clarke *et al.,* 2000). A schematic of the flow system used is given in Fig. 2a. In the first section of the flow system, reactant gases (CH_4, CO_2) were introduced into the mixing chamber at pressures from

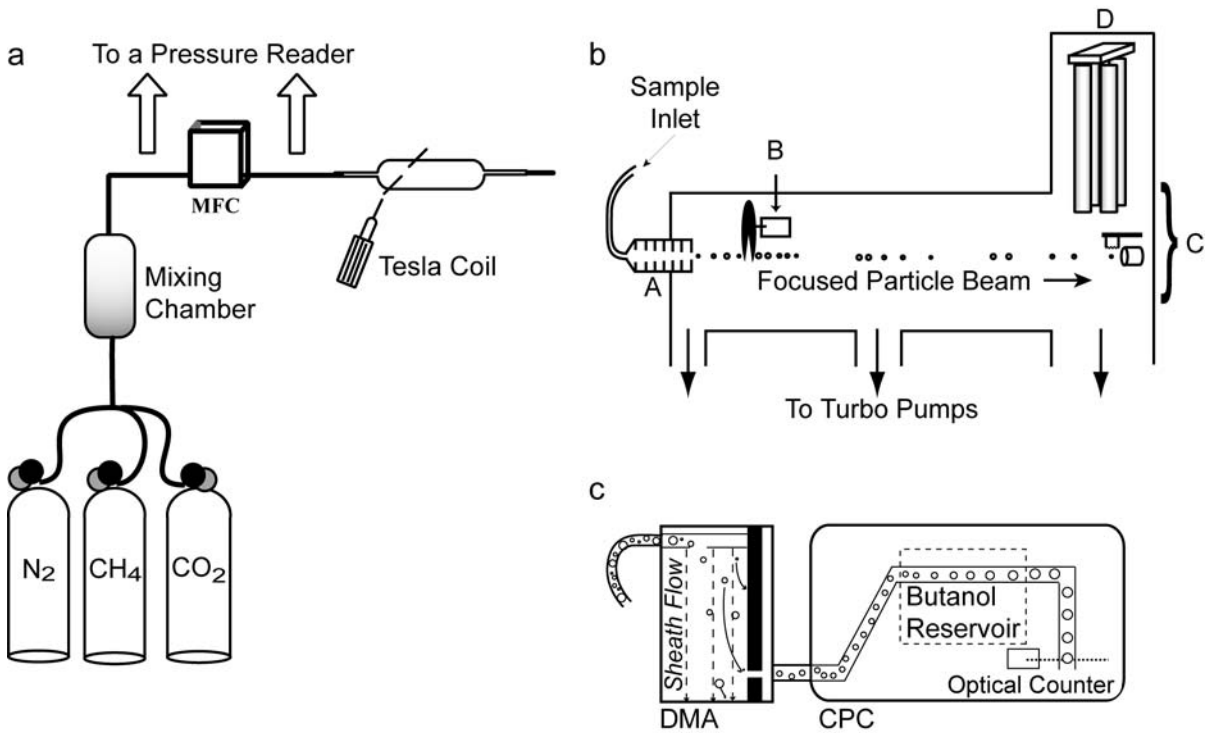

FIG. 2. a: A schematic diagram of the experimental setup used in all experiments. Particles are formed in the reaction cell and then flowed into one of the two analyzers. **b:** A schematic diagram for the AMS. Particles are focused into a tight particle beam using the aerodynamic focusing lens (A). A chopper (B) is used in time-of-flight mode to set a time zero for measuring particle velocity through the chamber. The flash vaporization and electron ionization region (C) produces ions that are sent into the quadrupole mass spectrometer (D) for analysis. **c:** A schematic diagram of the SMPS. The DMA uses the application of an electric field to select a particle size based on the mobility of a singly charged particle towards an electric rod and against the drag resistance of the sheath flow. The monodispersed particles are then flowed into the CPC, where they pass over a reservoir of butanol, which allows for particle condensation and growth. The aerosols are then detected and counted using light scattering from a He-Ne laser.

15.6 to 1,000 Torr as measured by an MKS (Wilmington, MA) Baratron® model 626A capacitance manometer. The mixing chamber was then pressurized with N_2 to approximately 15,600 Torr (21 bar), allowing for final mixing ratios of CH_4 and/or CO_2 in N_2 of 0.1–10% as monitored with a regulator gauge. The concentrations of the reactant gases in the N_2 were varied to simulate different possible atmospheric conditions. The various gas mixtures used in this study are outlined in Table 1. Sufficient time (>12 h) was allowed to ensure complete mixing of the gaseous species in the chamber, as determined in similar studies (Clarke *et al.*, 2000). The AMS was used to monitor the presence of the trace reactant gases during the experiments to check for mixture homogeneity.

After mixing, the gas was continuously flowed through the reaction cell using a Mykrolis (Billerica, MA) FC-2900 mass flow controller (MFC) (0–100 standard $cm^3\ min^{-1}$ capacity), providing control over the operating pressure and flow rate in the reaction cell. The reaction pressure in this study was held constant at 600 Torr, to allow for both proper instrument function and to ensure sufficient signal for analysis.

The data discussed in this paper are from studies performed using an electrical discharge from a Tesla coil. While the electrical discharge source has been widely used in simulations of Titan haze formation (for examples, see Khare *et al.*, 1981; McDonald *et al.*, 1994; McKay, 1996; Coll *et al.*, 1999), UV radiation would have been the main energy source for haze formation on the early Earth. In designing our experiment, however, we wished to take full advantage of the real-time measurement capabilities of the AMS, which requires a minimum of 0.1 $\mu g\ m^{-3}$ of material for detection. Studies utilizing a UV lamp to produce haze aerosols have required lengthy experiment times to accumulate usable amounts of haze material (Clarke *et al.*, 2000; Adamkovics and Boering, 2003), and we were concerned that we would not be able to produce the abundance of signal desired for the rapid analysis of the aerosols. Therefore, we chose to use the electrical discharge source, with which we have had prior experience, to ensure that we would produce sufficient signal to execute this novel analysis technique. Using the discharge also allows us to compare our results with most of the previous experiments, mentioned above, that also used a spark source.

The aerosol haze particles were formed in the reaction cell using the electrical discharge described. Because there was a possibility that varying the gas composition would lead to a change in the discharge energetics, temperature measurements of the gas surrounding the discharge were made for the gas mixtures to monitor the discharge power (Navarro-Gonzalez *et al.*, 1998). The discharge temperatures measured were the same, within error, and therefore we assumed the starting gas mixture did not affect discharge power. The haze particles, which were formed under short time scales (<10 min), were then flowed into the third section of the system for analysis.

The AMS, built by Aerodyne Research (Billerica) (Jayne *et al.*, 2000), obtains quantitative particle composition and size data without exposing aerosols to laboratory air. A schematic of the instrument is provided in Fig. 2b. The AMS operates in a mode that acquires averaged mass spectra of the bulk aerosol composition, as well as a time-of-flight mode in which individual particles are counted and mass size distributions are measured. The haze particles are directed into the AMS and focused as a particle beam using an aerodynamic focusing lens that transmits particles with aerody-

Table 1. Experimental Conditions for All Data Discussed in This Paper

C/O ratio	*[CH_4] (%)*	*[CO_2] (%)*	*[N_2] (%)*	*Analysis instrument*
—	1	0	99	AMS
5.5	1	0.1	98.9	AMS
1.5	1	0.5	98.5	AMS/SMPS
1	1	1	98	AMS/SMPS
0.95	1	1.1	97.9	AMS/SMPS
0.9	1	1.25	97.75	SMPS
0.8	1	1.67	97.33	SMPS
0.6	1	5	94	AMS/SMPS

All data shown are for experiments at 600 Torr total pressure.

namic diameters between approximately 20 nm and 1 μm. The beam is then expanded from approximately 2 mbar into a high vacuum time-of-flight chamber, which uses the size-dependent velocities to provide information on particle vacuum aerodynamic diameter (Jimenez *et al.,* 2003a,b). The particle vacuum aerodynamic diameter (D_{va}) is defined for the AMS as the diameter of a sphere of unit density that will reach the same terminal velocity in the AMS as the particle of interest. The particles are then flash-vaporized on a resistively heated surface held at approximately 450°C, and then ionized by bombardment of energetic electrons (70 eV). The ions are analyzed using a quadrupole mass spectrometer, manufactured by Balzers Instruments (Balzers, Liechtenstein). We calibrated the ionization and detection efficiency of the instrument using a known mass flux of monodispersed ammonium nitrate (NH_4NO_3) particles. The size calibration was performed at the operating pressure using calibrated polystyrene latex spheres. The calibration methods are discussed in more detail in Jayne *et al.* (2000). The data analysis program used for this instrument, including all signal conversions, has been described in detail in a previous publication (Allan *et al.,* 2003).

Additional experiments were performed using an SMPS in place of the AMS. This instrument was used to provide an independent technique with which to gather information regarding the size distribution of the haze aerosols produced in our experiments. The SMPS comprises a TSI (Shoreview, MN) model 3080 electrostatic classifier with a model 3081 differential mobility analyzer (DMA) and a condensation particle counter (CPC) (TSI 3022A). A schematic of this instrument is provided in Fig. 2c. The DMA applies an electric field to a flow of charged, polydispersed aerosols, and size-selects particles based on electrical mobility against the drag force of the sheath flow. The particle size measured by the DMA is a mobility diameter. Since particle shape affects the drag force of the aerosols, the mobility diameter depends on particle morphology rather than material density. The monodispersed particles are then flowed into the CPC, which counts each particle by light scattering. The DMA sheath flow was maintained at 3 L/min, and data points were taken over a particle diameter range of 14.3 to 673 nm. Because of experimental constraints, such as the gas flow rate and particle formation rate, we were unable to run the AMS and SMPS instruments simultaneously.

RESULTS

Figure 3 shows the aerosol mass spectra from experiments in which haze aerosols were synthesized in mixtures of various concentrations of CO_2 with 1% CH_4 in N_2 at 600 Torr. The mass spectrum shown in Fig. 3a contains no CO_2, and is representative of the signature for non-oxidized organic aerosols. This spectrum contains a large number of peaks with evenly spaced mass/charge (*m/z*) values, indicating long hydrocarbon chains, consistent with organics that comprise a variety of "families": branched and unbranched alkanes, alkenes, aromatics, and aliphatic nitriles and amines (McLafferty and Turecek, 1993). For complicated mixtures of organic molecules there are analysis techniques that group *m/z* values into series, separated by 14 amu (CH_2) units, to identify fragments of different functional groups from the mass spectrum (Dromey, 1976; McLafferty and Turecek, 1993). Applying this method to the mass spectrum in Fig. 3a, we find that the mass peaks for 27, 41, 55 and 29, 43, 57 are characteristic of alkyl chains. The mass peaks at 39, 53, 67 are representative of an alkene series, and the peaks seen at 77, 91, 105 are consistent with an aromatic series. These fragments are pieces of the larger, higher-mass chains that eventually form the aerosols. Particles are produced down to values as low as 1,000 ppmv of CH_4, a relevant mixing ratio for the early Earth (Pavlov *et al.,* 2000).

Figure 3b–d shows spectra for which increasing amounts of CO_2 in the reaction mixture alter the composition of the haze aerosols produced. As CO_2 was added, the total mass of particles decreased, and the chemical nature of the particles changed. Specifically, at C/O ratios <1, long-chain hydrocarbon formation decreased dramatically. This trend was observed in the region of the spectrum between 48 and 120 amu, where the intensity of fragments of long hydrocarbon chains decreased as CO_2 was increased.

In addition to total mass decreasing as CO_2 concentration is increased, the chemical composition of the aerosol changes. In particular, the ion peak at *m/z* 44 becomes a dominant peak in the spectra as the C/O ratio drops below unity. The *m/z* 44 peak may correspond to a carboxylic acid or other oxidized organic being produced at low C/O ratios. Other workers have found that for di- and polycarboxylic acids, the *m/z* 44 signal is more substantial in the AMS spectra than in the National Institute of Standards and Technology

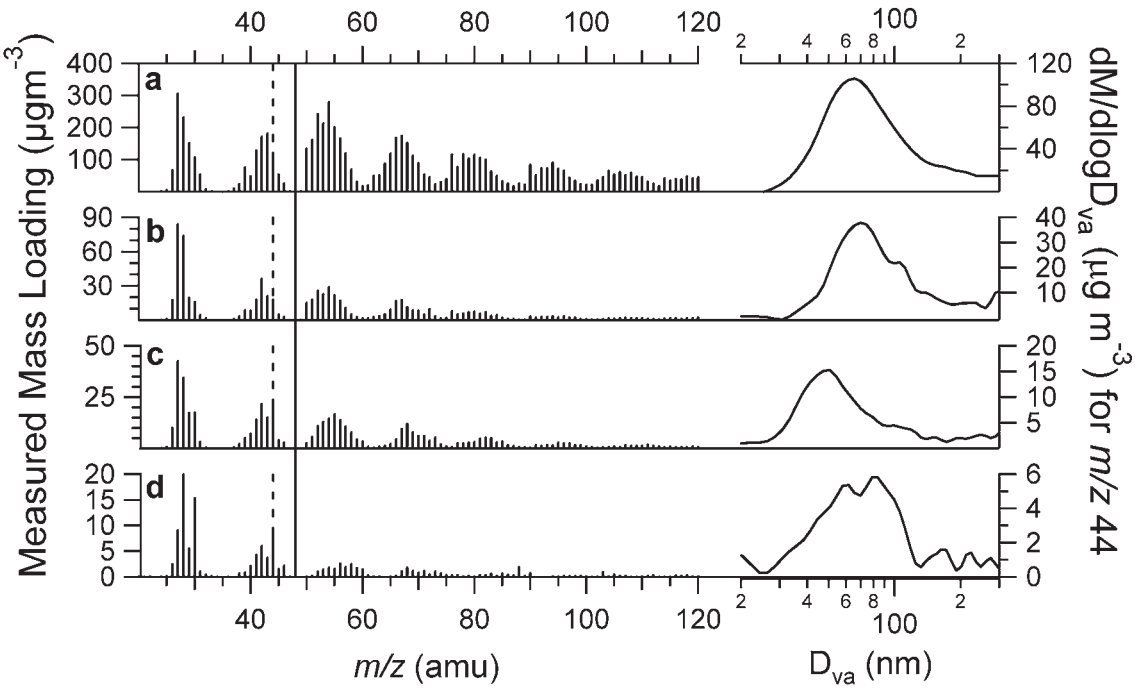

FIG. 3. Mass spectra of haze aerosols produced in various mixtures of increasing CO_2, as outlined in Table 1. Data to the right of the 48 amu marker are shown at 4× magnification of the scale to the left. **a:** No CO_2 incorporation. The mass fragment pattern is typical of non-oxidized organic aerosols. **b:** C/O ratio is 1.5. **c:** C/O ratio is 0.95. **d:** C/O ratio is 0.6. Particle size distributions for the mass peak at 44 amu, highlighted with black dashed lines, are shown to the right of the spectra. The particle signals, reported as lognormal mass distributions as a function of vacuum aerodynamic diameter (D_{va}), show that the 44 amu signal is derived from aerosols with diameters of approximately 60 nm. These distributions confirm that the fragment peak seen in the spectra is from molecules within the particles and not solely from gaseous CO_2.

standard library of mass spectra (Alfarra *et al.*, 2004). This is probably due to thermal decomposition of the molecules upon impact on the vaporizer, leading to an enhancement of the COO^+ fragment. The results obtained by Alfarra *et al.* (2004) for these substances are comparable to our data, indicating that the *m/z* 44 peak is a good marker for oxidized organics. As the C/O value decreases, this peak rises in prominence in the spectra, illustrating that the product molecules in the particle synthesis are becoming increasingly more oxidized. The mass peak at *m/z* 44 is also consistent with the CH_2NO^+ fragment, but in any case the peak is an indicator for oxygen incorporation. Particle size distributions from the AMS for *m/z* 44 signal are shown in Fig. 3. It can be seen that for all the C/O ratios studied, there is a distinct distribution mode at approximately 60 nm. This is too large a diameter to be the signal for a gas molecule, and therefore we conclude that the *m/z* 44 peak is not from gaseous CO_2, but rather is a fragment of a molecule in the haze aerosols. The mass peak at $m/z = 30$ has a similar observable effect within the mass spectra. The increasing prominence of this mass peak with CO_2 indicates that it is also an oxidized organic species, and it is consistent with the formation of an NO^+ fragment. Therefore, this peak may also be an indicator of the formation of nitrogen species.

Experiments in which the aerosol production was studied as a function of C/O ratio were also performed with the SMPS, and the volume size distributions are shown in Fig. 4. The data from the two techniques are compared in Fig. 5. Both data sets display a similar decrease in particle mass as the C/O ratio drops. It should be noted, however, that despite this decrease there is still significant particle production down to the lower limit of our C/O ratios at 0.6. Therefore, the particle production may be more ubiquitous than previously calculated by photochemical models,

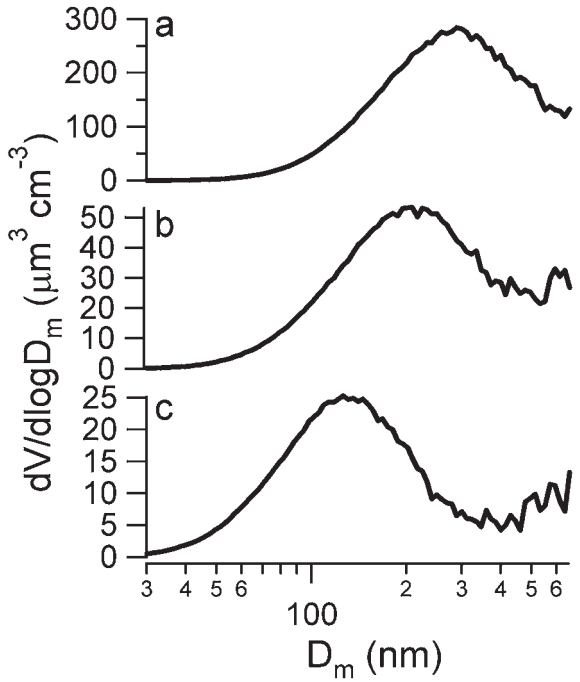

FIG. 4. Volume size distributions for particles measured in the SMPS as a function of mobility diameter (D_m). a: C/O ratio is 1.5. **b:** C/O ratio is 0.95. **c:** C/O ratio is 0.6.

which had assumed a cessation of polymerization below a C/O of unity (Zahnle, 1986; Pavlov *et al.*, 2001b).

DISCUSSION

Examination of the compositional evolution of the aerosols as a function of C/O ratio is explored in Fig. 6. In this figure, both the mass fragments at *m/z* 44 and 30 are compared with the total organic signal. The value for the total organic signal is calculated by integrating all of the product mass peaks in each mass spectrum, having made corrections for the gas background signals. Because *m/z* 44 is typically attributed to a COO^+ fragment for oxidized organics, we have used it as a marker for the degree of oxidation. Figure 6a is a plot of the ratio of (*m/z* 44)/total organics showing that adding CO_2 increases the ratio of (*m/z* 44)/total organics, consistent with the oxidation of the organic species in the particles. The change in the (*m/z* 44)/total organics ratio corresponds to a shift in the product formation from polymerization to oxidation, and correlates well to the decline in haze production with increasing CO_2. Figure 6b shows a plot of *m/z* 30 correlated to the total organic signal, which shows the same behavior as the plot in Fig. 6a. This indicates that the product peak at *m/z* 30 is likely that of an oxidized species, possibly NO^+ as previously mentioned.

In addition to information on the chemical composition of the aerosols, our experiment also provides insight into the particle morphology. The AMS and SMPS each measure the particle diameter in a different way, and by comparing these diameters we can obtain additional information about the physical characteristics of the aerosols. The SMPS measures mobility diameter (D_m), while the AMS measures the size of the aerosols as a vacuum aerodynamic diameter (D_{va}). Jimenez *et al*. (2003a,b) have shown that an effective particle density, ρ_{eff}, for spherical particles can be found by relating these two diameters:

$$\rho_{eff} = \rho_0 \frac{D_{va}}{D_m} \propto \frac{\rho_p}{\chi} \quad (1)$$

where ρ_0 is the unit density (1 g cm^{-3}), ρ_p is the material density of the particle, and χ is the dimensionless shape factor. Since the AMS and SMPS experiments were not done simultaneously, we cannot calculate an exact value for the

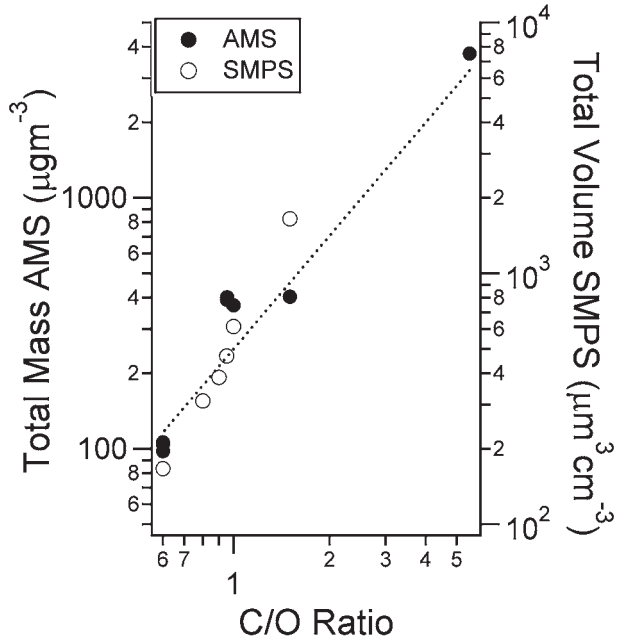

FIG. 5. Comparison of the haze aerosol mass produced as measured by both the AMS and the SMPS techniques. The dotted line shows an empirical kinetic fit to the AMS data of Product Mass (μg m^{-3}) = 250[C/O]$^{1.5}$.

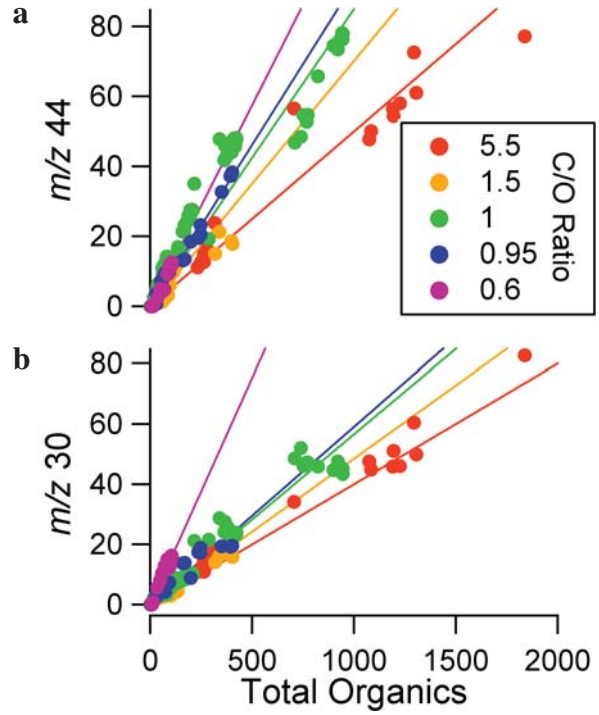

FIG. 6. Peak intensities of *m/z* values in the mass spectra of haze aerosols are compared with the total organic signal, colored as a function of the C/O ratio. a: Total mass produced at $m/z = 44$ compared with the total organic signal. The peak intensities for $m/z = 44$ have been corrected to remove the contribution from gaseous CO_2 in the starting gas mixture. **b:** The total mass produced at $m/z = 30$ compared with the total organic signal. Both mass peaks show a correlation between the relative peak intensity and the ratio of C/O, implying that the fragments are from oxidized species. The slopes of these ratios, shown with colored lines, increase with increasing CO_2. If these slopes are plotted as a function of C/O ratio, they show an exponential dependence with the equations of Slope (44/total organics) = $0.05 + (0.15)e^{(-1.35[\text{C/O ratio}])}$, and Slope (30/total organics) = $0.04 + (2.65)e^{(-5.35[\text{C/O ratio}])}$.

effective density from these data sets. However, taking into account the mode diameters of the particles as measured by both instruments shown in Figs. 3 and 4, we have determined approximate effective particle densities between 0.2 and 0.5 g cm^{-3}. A separate check was done using the comparison between total mass and total volume as shown in Fig. 5, yielding an effective density of approximately 0.5 g cm^{-3}.

These density values are very low compared with the material density for the organics believed to compose the aerosols, which are all around 0.8 g cm^{-3}, and models of Titan haze aerosols that have typically used a particle density of 1 g cm^{-3} (Toon *et al.*, 1992). Equation 1 shows that the ρ_{eff} is proportional to the material density but also depends on χ, which is equal to 1 for spherical particles, but is greater than 1 for non-spherical aerosols. A low effective density is characteristic of particles in which coagulation has led to the formation of non-spherical, lower-density structures (Jimenez *et al.*, 2003a,b). In regards to the haze layer on Titan, microphysical models matched to the optical properties of Titan's atmosphere have suggested that the particles are non-spherical aggregates of spherical monomers, and they are characterized as fractal particles (McKay *et al.*, 2001). Our results suggest that haze aerosols formed on the early Earth may also be fractal particles. Optical properties are largely dependent on shape; thus it would be extremely important to include the fractal shape information into a climate model that examines the properties of a haze layer on early Earth (Pavlov *et al.*, 2001a). Such a particle shape would explain the large discrepancy between the particle size measured by the AMS and the SMPS systems, and therefore the very low effective particle density reported above.

Here we would like to briefly discuss the effect that our choice of electrical discharge as the experimental energy source may have on the properties of the observed haze aerosols. A recent study by Tran *et al.* (2003) compared the optical and compositional properties of Titan analog particles produced using a UV source in their laboratory with those of previously mentioned experiments with discharge sources (see McKay, 1996). They found that the C/N ratio derived from elemental analysis was the most significant difference between these two types of aerosol particles, being much higher for particles formed with a UV source. This is most likely due to the higher energy input of the electrical discharge, which allows for the breaking of the N_2 bond, and thus a higher N incorporation into the haze molecules. The majority of UV light available in the Earth's atmosphere would not be of sufficient energy to break the N_2 bond, and therefore we expect the experiments described here to overestimate the amount of N in the aerosols.

Therefore, rather than focus on analysis of the N content of the aerosols, the main objective of this work has been to detect a particle formation threshold in atmospheres with mixtures of CO_2 and CH_4. We feel that this study has provided a satisfactory identification of the C/O ratios at which organic particle formation is still possible.

Since the discharge source is more energetic than UV, we may be observing an extreme for particle formation that will provide experimental boundaries for experiments using a UV source. Future experiments using this analytical method with UV light as the energy source will provide a systematic analysis of the C/O particle formation threshold on early Earth, and also of the effects of energy source on the chemical properties of the aerosols.

CONCLUSIONS

We have shown that particles are produced in a simulated atmosphere with CH_4 concentrations as low as 1,000 ppmv. This CH_4 level is sufficient to provide an early Earth greenhouse effect (Pavlov *et al.,* 2000), and thus haze particles might have formed on early Earth. We have also shown that a haze may still be produced in atmospheres with CO_2 in addition to CH_4. We have found that the decrease in haze production is directly proportional to the CO_2 concentration. Since there is no strict constraint on the average temperatures in the Archean, it is hard to estimate the exact CO_2 abundance in the ancient atmosphere and therefore the exact amount of haze produced. However, we have observed particle production even at the lowest C/O ratio reached in this study, which correlates to a CH_4/CO_2 ratio of 0.2. This suggests that a haze layer could still be maintained even if the Archean CO_2 concentration was as high as 5,000 ppmv. Fluctuations in the ancient climate would cause fluctuations in CH_4/CO_2 ratio (Pavlov *et al.,* 2001a), thus greatly affecting the level of haze production. However, our experiments suggest that some amount of haze should have been present over broad ranges of the possible CH_4 and CO_2 concentrations throughout most of the Archean. We have also observed that the aerosol particles produced appear to be fractal in nature, which is expected to have a large effect on the optical properties of the haze. Depending on the shielding capabilities of the aerosols, the haze layer may behave according to the feedback scheme proposed in Pavlov *et al.* (2001a).

In addition to the effects such a haze layer may have had on climate, it is also interesting to consider its interactions with the biosphere. Life, if present by the beginning of the Archean (Mojzsis *et al.,* 1996), would likely have influenced the evolution of the atmosphere (Kasting and Siefert, 2002). It has been suggested that microorganisms in the current atmosphere may contribute to the degradation of organic aerosols (Ariya *et al.,* 2002). Ariya *et al.* (2002) showed that airborne microorganisms are able to digest various dicarboxylic acids. These acids have functional groups and structural arrangements that are similar to the types of compounds we believe make up the haze aerosols when the environmental C/O ratio is low. Therefore, it is possible that the organic aerosols present in a haze layer on early Earth may have served as a source of food for some of the early biota. Microorganisms present during this time include anaerobic methanogens and cyanobacteria (Woese, 1987; Brocks *et al.,* 1999). These microorganisms contribute to the cycling of organic matter through a combined effort of fermentation and methanogenesis, thus producing methane (Zinder, 1993). While the hydrocarbon species produced at high C/O ratios may not be as edible, it is possible that if the haze aerosols were sufficiently oxidized, then the particles would have been able to serve as food for the fermenters (Ferry, 1993).

ACKNOWLEDGMENTS

This material is based upon work supported by the National Aeronautics and Space Administration under Grant NNG04GM42G issued through the Office of Space Science. Partial support was also received from the NASA Astrobiology Institute through the University of Colorado Center for Astrobiology and the National Science Foundation. MGT was supported by a fellowship through the NASA GSRP program and NASA Office of Space Science. DBC was supported by a GSRP fellowship through Ames Research Center.

ABBREVIATIONS

AMS, aerosol mass spectrometer; CPC, condensation particle counter; DMA, differential mobility analyzer; MFC, mass flow controller; SMPS, scanning mobility particle sizer; UV, ultraviolet.

REFERENCES

Adamkovics, M. and Boering, K.A. (2003) Photochemical formation rates of organic aerosols through time-re-

solved in situ laboratory measurements. *J. Geophys. Res.* 108, 5092–5105.

Alfarra, M.R., Coe, H., Allan, J.D., Bower, K.N., Boudries, H., Canagaratna, M.R., Jimenez, J.L., Jayne, J.T., Garforth, A., Li, S.M., and Worsnop, D.R. (2004) Characterization of urban and regional organic aerosols in the Lower Fraser Valley using two Aerodyne aerosol mass spectrometers. *Atmos. Environ.* 38, 5745–5758.

Allan, J.D., Jimenez, J.L., Williams, P.I., Alfarra, M.R., Bower, K.N., Jayne, J.T., Coe, H., and Worsnop, D.R. (2003) Quantitative sampling using an Aerodyne aerosol mass spectrometer—1. Techniques of data interpretation and error analysis. *J. Geophys. Res.* 108, 4090–4099.

Ariya, P.A., Nepotchatykh, O., Ignatova, O., and Amyot, M. (2002) Microbiological degradation of atmospheric organic compounds. *Geophys. Res. Lett.* 29, 2077–2080.

Brocks, J.J., Logan, G.A., Buick, R., and Summons, R.E. (1999) Archean molecular fossils and the early rise of eukaryotes. *Science* 285, 1033–1036.

Clarke, D.W., Joseph, J.C., and Ferris, J.P. (2000) The design and use of a photochemical flow reactor: A laboratory study of the atmospheric chemistry of cyanoacetylene on Titan. *Icarus* 147, 282–291.

Coll, P., Coscia, D., Gazeau, M.C., de Vanssay, E., Guillemin, J.C., and Raulin, F. (1995) Organic chemistry in Titan's atmosphere: New data from laboratory simulations at low temperature. *Adv. Space Res.* 16, 93–103.

Coll, P., Coscia, D., Smith, N., Gazeau, M.C., Ramirez, S.I., Cernogora, G., Israel, G., and Raulin, F. (1999) Experimental laboratory simulation of Titan's atmosphere: Aerosols and gas phase. *Planet. Space Sci.* 47, 1331–1340.

de Vanssay, E., McDonald, G.D., and Khare, B.N. (1999) Evidence from scanning electron microscopy of experimental influences on the morphology of Triton and Titan tholins. *Planet. Space Sci.* 47, 433–440.

Dromey, R.G. (1976) Simple index for classifying mass-spectra with applications to fast library searching. *Anal. Chem.* 48, 1464–1469.

Ferry, J.G. (1993) Fermentation of acetate. In *Methanogenesis: Ecology, Physiology, Biochemistry, and Genetics,* edited by J.G. Ferry, Chapman and Hall, New York, pp. 305–334.

Jayne, J.T., Leard, D.C., Zhang, X., Davidovits, P., Smith, K.A., Kolb, C.E., and Worsnop, D.R. (2000) Development of an aerosol mass spectrometer for size and composition analysis of submicron particles. *Aerosol Sci. Technol.* 33, 49–70.

Jimenez, J.L., Bahreini, R., Cocker, D.R., Zhuang, H., Varutbangkul, V., Flagan, R.C., Seinfeld, J.H., O'Dowd, C., and Hoffmann, T. (2003a) New particle formation from photooxidation of diiodomethane (CH_2I_2). *J. Geophys. Res.* 108, 4318–4342.

Jimenez, J.L., Bahreini, R., Cocker, D.R., Zhuang, H., Varutbangkul, V., Flagan, R.C., Seinfeld, J.H., O'Dowd, C., and Hoffmann, T. (2003b) Correction to "New particle formation from photooxidation of diiodomethane (CH_2I_2)." *J. Geophys. Res.* 108, 4733.

Kasting, J.F. (1993) Earth's early atmosphere. *Science* 259, 920–926.

Kasting, J.F. (1997) Planetary atmospheres: Warming early Earth and Mars. *Science* 276, 1213–1215.

Kasting, J.F. and Siefert, J.L. (2002) Life and the evolution of Earth's atmosphere. *Science* 296, 1066–1068.

Khare, B.N., Sagan, C., Zumberge, J.E., Sklarew, D.S., and Nagy, B. (1981) Organic-solids produced by electrical-discharge in reducing atmospheres: Tholin molecular analysis. *Icarus* 48, 290–297.

Khare, B.N., Sagan, C., Arakawa, E.T., Suits, F., Callcott, T.A., and Williams, M.W. (1984) Optical constants of organic tholins produced in a simulated Titanian atmosphere: From soft x-ray to microwave frequencies. *Icarus* 60, 127–137.

Khare, B.N., Bakes, E.L.O., Imanaka, H., McKay, C.P., Cruikshank, D.P., and Arakawa, E.T. (2002) Analysis of the time-dependent chemical evolution of Titan haze tholin. *Icarus* 160, 172–182.

Kiehl, J.T. and Dickinson, R.E. (1987) A study of the radiative effects of enhanced atmospheric CO_2 and CH_4 on early Earth surface temperatures. *J. Geophys. Res.* 92, 2991–2998.

Kress, M.E. and McKay, C.P. (2004) Formation of methane in comet impacts: Implications for Earth, Mars, and Titan. *Icarus* 168, 475–483.

McDonald, G.D., Thompson, W.R., Heinrich, M., Khare, B.N., and Sagan, C. (1994) Chemical investigation of Titan and Triton tholins. *Icarus* 103, 137–145.

McKay, C.P. (1996) Elemental composition, solubility, and optical properties of Titan's organic haze. *Planet. Space Sci.* 44, 741–747.

McKay, C.P., Lorenz, R.D., and Lunine, J.I. (1999) Analytic solutions for the antigreenhouse effect: Titan and early Earth. *Icarus* 137, 56–61.

McKay, C.P., Coustenis, A., Samuelson, R.E., Lemmon, M.T., Lorenz, R.D., Cabane, M., Rannou, P., and Drossart, P. (2001) Physical properties of the organic aerosols and clouds on Titan. *Planet. Space Sci.* 49, 79–99.

McLafferty, F.W. and Turecek, F. (1993) *Interpretation of Mass Spectra,* University Science Books, Sausalito, CA.

Miller, S.L. and Schlesinger, G. (1984) Carbon and energy yields in prebiotic syntheses using atmospheres containing CH_4, CO and CO_2. *Origins Life Evol. Biosphere* 14, 83–90.

Mojzsis, S.J., Arrhenius, G., McKeegan, K.D., Harrison, T.M., Nutman, A.P., and Friend, C.R.L. (1996) Evidence for life on Earth before 3,800 million years ago. *Nature* 384, 55–59.

Navarro-Gonzalez, R., Romero, A., and Honda, Y. (1998) Power measurements of spark discharge experiments. *Origins Life Evol. Biosphere* 28, 131–153.

Newman, M.J. and Rood, R.T. (1977) Implications of solar evolution for Earth's early atmosphere. *Science* 198, 1035–1037.

Pavlov, A.A., Kasting, J.F., Brown, L.L., Rages, K.A., and Freedman, R. (2000) Greenhouse warming by CH_4 in the atmosphere of early Earth. *J. Geophys. Res.* 105, 11981–11990.

Pavlov, A.A., Kasting, J.F., Eigenbrode, J.L., and Freeman, K.H. (2001a) Organic haze in Earth's early atmosphere: The source of low-^{13}C late Archean kerogens? *Geology* 29, 1003–1006.

Pavlov, A.A., Brown, L.L., and Kasting, J.F. (2001b) UV-shielding of NH_3 and O_2 by organic hazes in the Archean atmosphere. *J. Geophys. Res.* 106, 23267–23287.

Ramirez, S.I., Coll, P., da Silva, A., Navarro-Gonzalez, R., Lafait, J., and Raulin, F. (2002) Complex refractive index of Titan's aerosol analogues in the 200–900 nm domain. *Icarus* 156, 515–529.

Rye, R., Kuo, P.H., and Holland, H.D. (1995) Atmospheric carbon dioxide concentrations before 2.2-billion years ago. *Nature* 378, 603–605.

Sagan, C. and Chyba, C. (1997) The early faint sun paradox: Organic shielding of ultraviolet-labile greenhouse gases. *Science* 276, 1217–1221.

Sagan, C. and Khare, B.N. (1979) Tholins: Organic chemistry of interstellar grains and gas. *Nature* 277, 102–107.

Sagan, C. and Mullen, G. (1972) Earth and Mars—evolution of atmospheres and surface temperatures. *Science* 177, 52–56.

Thompson, W.R., Henry, T.J., Schwartz, J.M., Khare, B.N., and Sagan, C. (1991) Plasma discharge in $N_2 + CH_4$ at low pressures: Experimental results and applications to Titan. *Icarus* 90, 57–73.

Thompson, W.R., McDonald, G.D., and Sagan, C. (1994) The Titan haze revisited—magnetospheric energy-sources and quantitative tholin yields. *Icarus* 112, 376–381.

Toon, O.B., McKay, C.P., Griffith, C.A., and Turco, R.P. (1992) A physical model of Titan's aerosols. *Icarus* 95, 24–53.

Toublanc, D., Parisot, J.P., Brillet, J., Gautier, D., Raulin, F., and McKay, C.P. (1995) Photochemical modeling of Titan's atmosphere. *Icarus* 113, 2–26.

Tran, B.N., Joseph, J.C., Ferris, J.P., Persans, P.D. and Chera, J.J. (2003) Simulation of Titan haze formation using a photochemical flow reactor—the optical constants of the polymer. *Icarus* 165, 379–390.

Woese, C.R. (1987) Bacterial evolution. *Microbiol. Rev.* 51, 221–271.

Zahnle, K.J. (1986) Photochemistry of methane and the formation of hydrocyanic acid (HCN) in the Earth's early atmosphere. *J. Geophys. Res.* 91, 2819–2834.

Zinder, S.H. (1993) Physiological ecology of methanogens. In *Methanogenesis: Ecology, Physiology, Biochemistry, and Genetics,* edited by J.G. Ferry, Chapman and Hall, New York, pp. 128–206.

Address reprint requests to:
Dr. Margaret A. Tolbert
Department of Chemistry and Biochemistry and
Cooperative Institute for Research
in Environmental Sciences
University of Colorado at Boulder
Campus Box 216
Boulder, CO 80309-0216

E-mail: tolbert@cires.colorado.edu